

Synthesis and Characterization of New Intermetallic Compounds $M_3(\text{AsTe}_3)_2$ (M=Cr, Fe, Co)

Jin-Seung Jung*, Hyun Hak Kim, Seog Gu Kang, Weon-Sik Chae, Don Kim[†], and Sung Han Lee[‡]

Department of Chemistry, Kangnung National University, Kangnung 210-702, Korea

[†]Department of Chemistry, Pukyong National University, Pusan 608-737, Korea

[‡]Department of Chemistry, Yonsei University, Wonju 220-710, Korea

Received August 2, 1997

The new amorphous intermetallic compounds, $M_3(\text{AsTe}_3)_2$ (M=Cr, Co, Fe), were synthesized by the precipitation reaction of the Zintl anion AsTe_3^{3-} with the divalent transition metal halides in aqueous solution and analyzed by EDS equipped with SEM and PIXE. The empirical formula of the specimens was found to be $\text{Fe}_{3.0}\text{As}_{1.8}\text{Te}_{5.9}$, $\text{Co}_{3.0}\text{As}_{2.1}\text{Te}_{6.5}$, and $\text{Cr}_{3.0}\text{As}_{2.0}\text{Te}_{6.9}$ by the quantitative elemental analysis. The dc specific resistivity of the materials was measured as a function of temperature in the range from 20 to 300 K, in which their resistivities were decreased with increasing temperature, indicating the specimens to be semiconductors. The resistivity of $\text{Cr}_3(\text{AsTe}_3)_2$ was largely dependent on temperature, while those of $\text{Co}_3(\text{AsTe}_3)_2$ and $\text{Fe}_3(\text{AsTe}_3)_2$ were only slightly dependent on temperature. To characterize the spin glass state of the specimens, the ac and dc magnetic susceptibility were measured and it was found that $\text{Co}_3(\text{AsTe}_3)_2$ and $\text{Fe}_3(\text{AsTe}_3)_2$ undergo a transition to a spin glass state at 6 K and 38 K, respectively. Magnetization data are reported as both thermal remanent magnetization (TRM) and isothermal remanent magnetization (IRM) as a function of magnetizing field and temperature.

Introduction

The coordination chemistry of metal sulfides and metal tellurides has been extensively investigated, due in part to their importance in industrial and biological processes.¹ During the last decade, several heteropolyanions of group 15 and tellurium have been synthesized by various techniques. $[\text{As}_{11}\text{Te}]^{3-}$ was obtained by the dissolution of appropriate alloys with alkali metals in ethylenediamine,² followed by the complexation of the alkali cation by macrocyclic [2,2,2]¹⁻-cryptand according to the procedure described by Corbett.³ Haushalter also synthesized $[\text{As}_{10}\text{Te}_3]^{2-}$ by reduction of polychalcogenates with an alkali metal in ethylenediamine.⁴ Recently, a more elegant procedure was proposed by Haushalter who prepared the $[\text{Sb}_4\text{Te}_4]^{4-}$, $[\text{Sb}_6\text{Te}_6]^{3-}$ and $[\text{Sb}_6\text{Te}_9]^{4-}$ anions by using an electrochemical procedure.⁵ We have previously found K_3SbTe_3 compound that is discrete molecular structure to form an ionic solution in polar solvents.⁶ In recent years, we have studied the amorphous intermetallic compounds using the MTe_3^{3-} (M=Sb, Ga) Zintl phase as precursor.⁷ Amorphous solids differ from crystalline ones in that they lack the long-range translational order characteristic of crystalline solids. This affects the optical, electronic and magnetic properties of the solids. These unique characteristics of amorphous materials have suggested potential applications in electronics, photovoltaics, catalysis, and optical and magnetic material.⁸ In this report, we describe the synthesis and characterization of new amorphous magnetic materials, $M_3(\text{AsTe}_3)_2$ (M=Cr, Fe, Co), which are produced from the reaction of the Zintl phase material, K_3AsTe_3 , with MCl_2 in an aqueous solution.

Experimental

Synthesis

Due to the air sensitivity of the materials used in these

reactions, all manipulations were carried out in an argon-filled glovebox containing less than 1 ppm of oxygen.

K_3AsTe_3 . The ternary Zintl material K_3AsTe_3 was prepared by direct combination of the elements. A dry quartz tube was charged with 0.12 g of K (3 mmol), 0.75 g of As (1 mmol), and 0.38 g of Te (3 mmol). The sample quartz tube was evacuated at a pressure of approximately 1×10^{-3} Torr for 1.5 hr and then sealed under vacuum. The sample tube was placed inside a larger diameter tube, which was similarly evacuated and sealed. The outer tube was used to prevent air contamination in the event that the inner tube is fractured during cooling. The sample was heated at 640 °C in an automatic control furnace for 20 hr, then cooled to ambient temperature over a 48-hr period and a metallic dark crystalline product was obtained.

$M_3(\text{AsTe}_3)_2$ (M=Cr, Fe, Co). The transition metal arsenic tellurides were prepared by the reaction of K_3AsTe_3 with transition metal halides. In a typical preparation, while stirring the MX_2 solution (25 mL, 0.1 M), a stoichiometric quantity of the K_3AsTe_3 solution (20 mL, 0.05 M) was slowly added. A fine black precipitate was immediately formed, separated by suction filtration, washed with degassed water and acetone, and dried overnight under vacuum. All samples were treated as air-sensitive in the course of physical measurements to prevent possible decomposition.

Elemental Analysis

The presence of the three elements in each sample and the homogeneity of each sample were confirmed with an EDS equipped with Jeol 6400 scanning electron microscope and Tandem 1.7 MV accelerator PIXE. The quantitative elemental analysis for these materials was carried out on a IL-S-12AA spectrometer. The atomic absorption standards were purchased from John-Matthey. The empirical formula determined for these materials gave the following chemical compositions: $\text{Fe}_{3.0}\text{As}_{1.8}\text{Te}_{5.9}$; $\text{Co}_{3.0}\text{As}_{2.1}\text{Te}_{6.5}$; $\text{Cr}_{3.0}\text{As}_{2.0}\text{Te}_{6.9}$.

Resistivity Measurement

Resistivity measurement for the materials was performed on pressed pellet over the temperature range 20-300 K using the van der Pauw technique. The pressed pellets were made under a pressure of 16000 psi. Electrical contact to the sample was made using gold wires attached with silver paint. The current was supplied by a Keithley Model 224 programmable current source and the voltage drop across the sample was measured with a Keithley Model 181 digital nanovoltmeter.

Magnetism

dc Magnetic Susceptibility. The magnetic susceptibility and magnetization were measured with a Quantum Design MPMS-5S SQUID susceptometer. Measurement and calibration techniques have been reported elsewhere. Three types of experiments were conducted: dc magnetic susceptibility (M/H), thermal remanent magnetization (TRM), and isothermal remanent magnetization (IRM), each as a function of field or temperature. The TRM experiment involves cooling the sample in an applied magnetic field and then measuring the remanent at zero magnetic field. The IRM experiment, on the other hand, involves cooling the sample in zero field and then applying a magnetic field.

ac Magnetic Susceptibility. The ac magnetic susceptibility was recorded on samples that were taken from the same synthetic batch used for the dc measurement and the data were recorded on a variable-frequency mutual inductance instrument. The operation and calibration of this instrument are described elsewhere. Both the in-phase component χ' and the out-of-phase component χ'' of the magnetic susceptibility at zero field were recorded at 100 Hz over the temperature range from 2 to 30 K.

Results and Discussion

For several years, we have been interested in the preparation and characterization of the amorphous intermetallic compounds.⁸ These materials are prepared using Zintl phase as precursor. Because the Zintl phase itself exhibits a very large distribution of charges that allows the Zintl material to exhibit salt like solubility properties in many polar solvents. Recent studies of the material containing metathesis products of these compounds have shown them to exhibit spin glass behavior, unusual photomagnetic effects, a wide range of electrical resistivities and catalytic properties.⁷ To continue the search for ternary amorphous intermetallic chalcogenide compounds, we have extended our study to $M_3(\text{AsTe}_3)_2$ ($M=\text{Cr, Fe, Co}$). The magnetic measurements of these materials show the $\text{Co}_3(\text{AsTe}_3)_2$ and $\text{Fe}_3(\text{AsTe}_3)_2$ to have a spin glass character. Figure 1 shows both in-phase magnetic susceptibility (χ') and the out-of-phase magnetic susceptibility (χ'') of $\text{Co}_3(\text{AsTe}_3)_2$ measured at 100 Hz and zero magnetic field. The in-phase magnetic ac susceptibility (χ') exhibits a sharp maximum with at approximately 6 K. The dc magnetic susceptibility results for $\text{Co}_3(\text{AsTe}_3)_2$ in the temperature range of 2 K to 300 K are presented in Figure 2 as the plot of the reciprocal susceptibility vs. temperature. The parameters from least-square fits of the temperature dependence of $1/\chi$ above 50 K to Curie-Weiss equation are $\theta = -14$ K. Usually, a sharp peak at a well-defined tem-

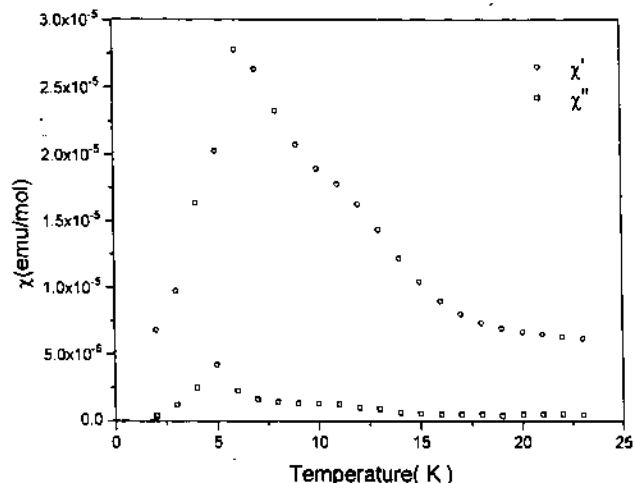


Figure 1. The temperature dependence of ac magnetic susceptibility measured at 100 Hz for $\text{Co}_3(\text{AsTe}_3)_2$.

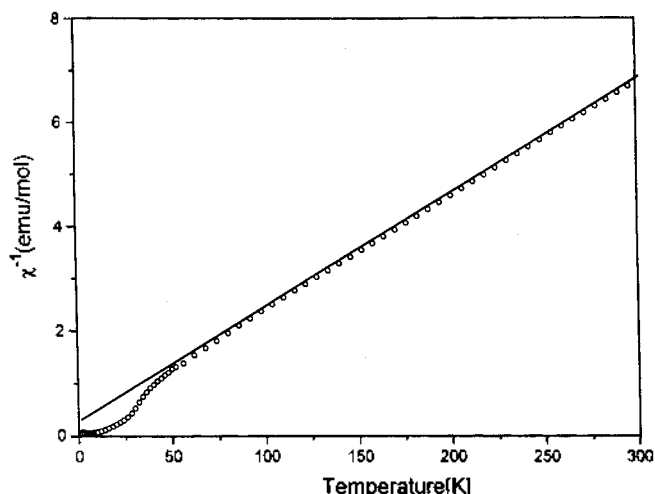


Figure 2. Temperature dependence of inverse molar susceptibility for $\text{Co}_3(\text{AsTe}_3)_2$. The solid line represents the Curie-Weiss fit.

perature called the freezing temperature T_f is observed in the ac susceptibility curve of the spin glass materials. The sharper peak in χ' occurs at lower temperatures and corresponds to the anomaly observed in the dc magnetic measurements. Figure 3 illustrates temperature dependence of magnetic susceptibility of $\text{Co}_3(\text{AsTe}_3)_2$ for field cooled and zero field cooled experiments at low temperatures. The maximum that is observed in the zero field cooled magnetic susceptibility data and absent in the field cooled ones is an evidence that $\text{Co}_3(\text{AsTe}_3)_2$ exists in a spin glass state with a freezing temperature of about 6 K. However, if the temperature approaches T_f , the susceptibility becomes more Curie-like. Below T_f the species are blocked, and the system is trapped in a highly irreversible, metastable state. The effect of an applied field below T_f is antiferromagnetic like with remanence. The dc data were measured in an applied magnetic field, while the ac data were measured at zero field condition. This could account for some of the apparent discrepancy between the ac and dc magnetic susceptibility data.

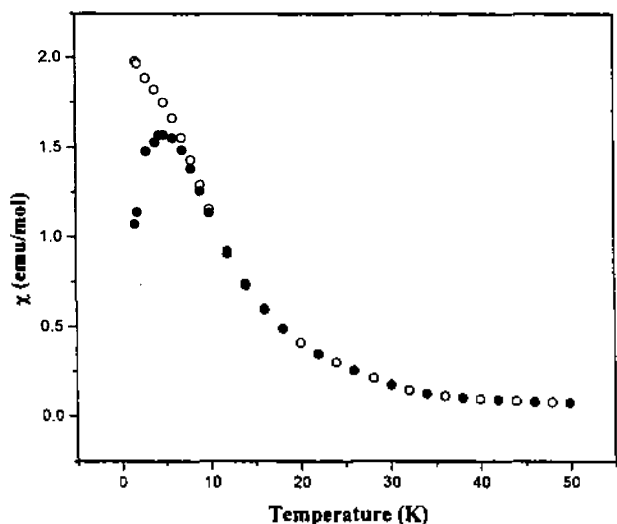


Figure 3. Plot of the magnetic susceptibility of $\text{Co}_3(\text{AsTe}_3)_2$ as a function of temperature measured at 1 kG (open circle: field cooling, dot: zero field cooling).

The same type of behavior has also been observed in $\text{Fe}_3(\text{AsTe}_3)_2$ as shown in Figure 4, but it has a high spin glass freezing temperature of about 38 K. The another important supporting experiment for the characterization of the spin glass state is the analysis of the field dependence of the isothermal remanent magnetization (IRM) and thermal remanent magnetization (TRM). The results of these experiments on $\text{Fe}_3(\text{AsTe}_3)_2$ are illustrated in Figure 5. A hump in the TRM curve has been observed in many spin glasses and is characteristic of the spin-glass state.¹⁰ Such a hump is apparent in the field dependent plot of the TRM data in Figure 5. The effect seen for the TRM is greatly enhanced by performing the experiment at lower temperatures, whereas the IRM is little affected by temperature. This is shown in Figure 6 where both TRM and IRM at an applied field of 1 kG are plotted as a function of temperature. The TRM and IRM curves merge near 38 K, the freezing point, which agrees with the susceptibility data at zero field cooling and field cooling.

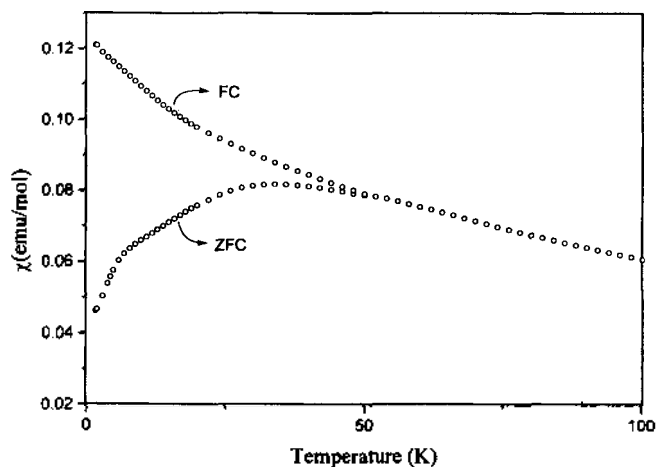


Figure 4. Plot of the magnetic susceptibility of $\text{Fe}_3(\text{AsTe}_3)_2$ as a function of temperature measured at a field of 1 kG (open circle: field cooling, dot: zero field cooling).

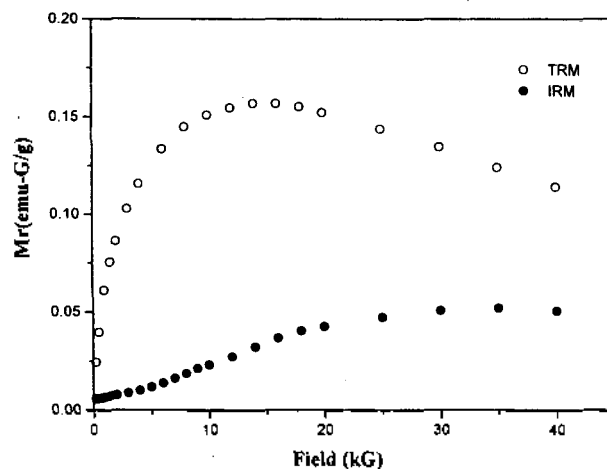


Figure 5. A plot of the IRM and TRM as a function of the magnetization field for $\text{Fe}_3(\text{AsTe}_3)_2$ at 6 K (open circle: TRM, dot: IRM).

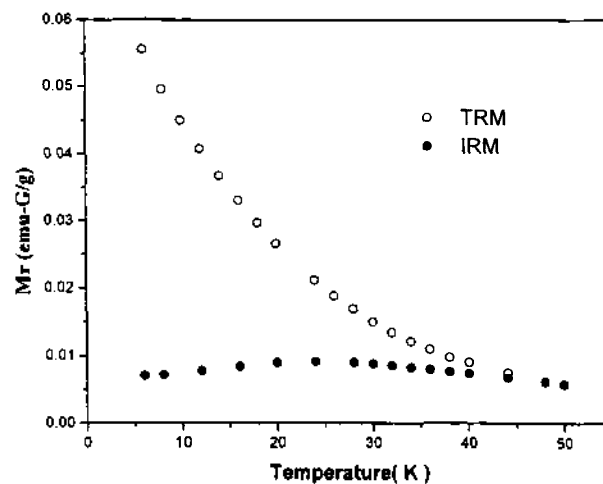


Figure 6. A plot of IRM and TRM as a function of temperature for $\text{Fe}_3(\text{AsTe}_3)_2$ at a remanent-inducing magnetic field of 1 kG.

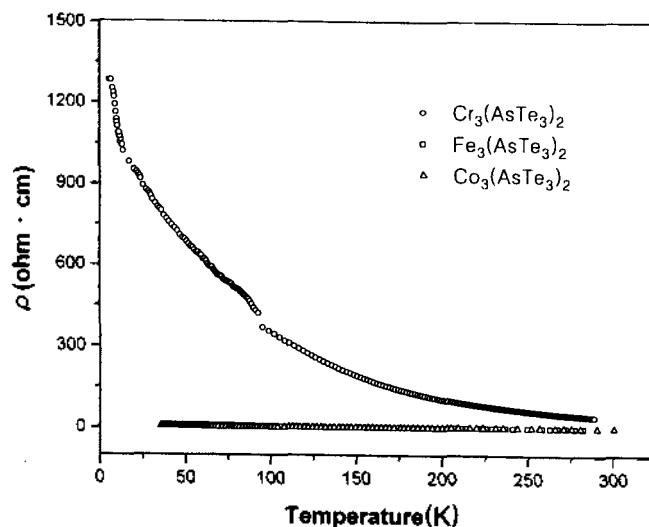


Figure 7. Temperature dependence of the specific resistivity for $M_3(\text{AsTe}_3)_2$ ($M=\text{Cr, Fe, Co}$).

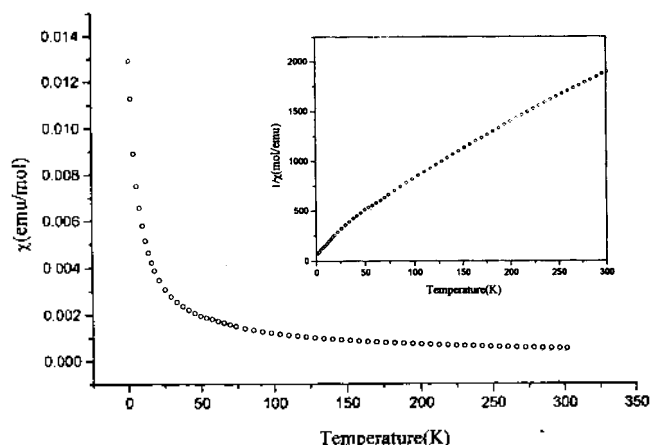


Figure 8. Temperature dependence of the inverse magnetic susceptibility and magnetic susceptibility for $\text{Cr}_3(\text{AsTe}_3)_2$.

The temperature dependence of the resistivity for $\text{M}_3(\text{AsTe}_3)_2$ is shown in Figure 7. It has a value of $4.32 \times 10^1 \Omega \text{ cm}$ for $\text{Cr}_3(\text{AsTe}_3)_2$, $3.67 \times 10^{-1} \Omega \text{ cm}$ for $\text{Fe}_3(\text{AsTe}_3)_2$, $3.41 \times 10^{-1} \Omega \text{ cm}$ for $\text{Co}_3(\text{AsTe}_3)_2$ at 300 K. The Fe, Co, and Cr analogues exhibit a negative temperature coefficient ($d\rho/dT$) throughout the temperature range investigated, indicating semiconductivity. The resistivity of $\text{Cr}_3(\text{AsTe}_3)_2$ is significantly larger than the other materials in this series, for example, three orders larger than that of $\text{Fe}_3(\text{AsTe}_3)_2$ and $\text{Co}_3(\text{AsTe}_3)_2$. The resistivities of $\text{Fe}_3(\text{AsTe}_3)_2$ and $\text{Co}_3(\text{AsTe}_3)_2$ are only slightly affected by temperature. An analysis of the data reveals that the $\text{Cr}_3(\text{AsTe}_3)_2$ has an estimated activation energy of 0.029 eV, based on the slope of the least-squares fit of the $\log \rho$ vs. $1/T$ plot. In Figure 8 the magnetic susceptibility data shows that the compound exhibits Curie-Weiss paramagnetism. At lower temperatures the magnetic susceptibility begins to deviate from Curie-Weiss law, but there is no characteristic magnetic anomaly to allow a precise determination of the nature of the magnetic coupling.

Acknowledgment. This paper was supported by

NON DIRECTED RESEARCH FUND, Korea Research Foundation, 1996.

References

- (a) Muler, A.; Diemann, E. *Adv. Inorg. Chem.* **1987**, *31*, 89. (b) Coucouvanis, M.; Hydjikyriacou, A.; Draganjac, M.; Kanatzidis, M.; Heperuma, O. *Polyhedron* **1986**, *5*, 349. (c) Harmer, M. A.; Halbert, T. R.; Pan, W.-H.; Coyle, C. L.; Cohen, S. A.; Stiefel, E. I. *Polyhedron* **1986**, *5*, 314. (d) Lee, S. C.; Holm, R. H. *Angew. Chem., Int. Ed. Engl.* **1990**, *29*, 840.
- Belin, C.; Mercier, H. *J. Chem. Soc., Chem. Commun.* **1987**, 190.
- Corbett, J. D.; Edwards, P. A. *J. Am. Chem. Soc.* **1977**, *99*, 3313.
- Haushalter, R. C. *J. Chem. Soc., Chem. Commun.* **1987**, 196.
- (a) Warren, C. J.; Ho, D. M.; Haushalter, R. C.; Bocarsly, A. B. *Angew. Chem., Int. Ed. Engl.* **1993**, *32*, 111646. (b) Warren, C. J.; Dbingra, S. S.; Ho, D. M.; Haushalter, R. C.; Bocarsly, A. B. *Inorg. Chem.* **1994**, *33*, 2709.
- Jung, J.-S.; Stevens, E. D.; O'Connor, C. J. *J. Solid State Chem.* **1991**, *94*, 362.
- (a) Jung, J.-S.; Ren, L.; O'Connor, C. J. *J. Mater. Chem.* **1992**, *2*, 829. (b) Jung, J.-S.; Wu, B.; Ren, L.; O'Connor, C. J. *J. Appl. Phys.* **1993**, *73*, 5463. (c) Jung, J.-S.; Wu, B.; Ren, L.; Tang, J.; Ferre, J.; Jamet, J.; O'Connor, C. J. *J. Mater. Res.* **1994**, *9*, 909.
- (a) Zallen, R. In *The Physics of amorphous Solids*; Wiley Sci.: New York, 1983. (b) Moorjani, K and Coey, J. M. D. In *Magnetic Glasses*; Elsevier Pub.: Amsterdam, 1985. (c) Lee, S. H.; Jung, J.-S.; Kim, H. H.; Kang, S. K.; Jung, D. W. *Bull. Korean Chem. Soc.* **1996**, *17*, 541.
- O'Connor, C. J.; Jung, J.-S.; Zhang, J. H. In *Chemistry, Structure, and Bonding of Zintl Phases and Ions*; VCR publishers: New York, 1996; p 275.
- Aharoni, A.; Wohlfarth, E. P. *J. Appl. Phys.* **1984**, *6*, 55.